NASA Technical Memorandum 101553

INTEGRATED AERODYNAMIC/DYNAMIC OPTIMIZATION
OF HELICOPTER ROTOR BLADES

Aditi Chattopadhyay, Joanne L. Walsh, and Michael F. Riley

February 1989

National Aeronautics and
Space Administration

Langley Research Center
Hampton, Virginia 23665-5225

Integrated Aerodynamic/Dynamic Optimization of Helicopter Rotor Blades

by

Aditi Chattopadhyay*
Analytical Services & Materials, Inc.
Hampton, Virginia 23666

Joanne L. Walsh**
NASA Langley Research Center
Hampton, Virginia 23665

and

Michael F. Riley***
Planning Research Corporation
Hampton, Virginia 23666

Abstract

In this paper, an integrated aerodynamic/dynamic optimization procedure is used to minimize blade weight and 4 per rev vertical hub shear for a rotor blade in forward flight. The coupling of aerodynamics and dynamics is accomplished through the inclusion of airloads which vary with the design variables during the optimization process. Both single and multiple objective functions are used in the optimization formulation. The 'Global Criteria Approach' is used to formulate the multiple objective optimization and results are compared with those obtained by using single objective function formulations. Constraints are imposed on natural frequencies, autorotational inertia and centrifugal stress. The program CAMRAD is used for the blade aerodynamic and dynamic analyses and the program CONMIN is used for the optimization. Since the spanwise and the azimuthal variations of loading are responsible for most rotor vibration and noise, the vertical airload distributions on the blade, before and after optimization, are compared. The total power required by the rotor to produce the same amount of thrust for a given area are also calculated before and after optimization. Results of this study indicate that integrated optimization can significantly reduce the blade weight and the hub shear as well as the amplitude of the vertical airload distributions on the blade and the total power required by the rotor.

Nomenclature

c	chord
f_3, f_4, f_5, f_6	natural frequencies of first four coupled elastic modes
g	constraint function
k	principle radius of gyration
k_{xx}, k_{yy}	radius of gyration about reference axes
s	area solidity
w_j	nonstructural weight per unit length at j^{th} node
x, y, z	reference axes
$\hat{y}_i$	distance from the root to the center of the i^{th} segment
A	box beam cross sectional area
AI	autorotational inertia
C_P	power coefficient
E	Young's modulus
EI_{xx}, EI_{zz}	bending stiffnesses
$F, \hat{F}$	objective functions
FS	factor of safety
F_p	blade vertical airload
F_z	amplitude of 4/rev vertical hub shear
GJ	torsional stiffness
I_{xx}, I_{zz}	principal area moments of inertia about reference axes
L_i	length of i^{th} segment
M_i	mass of i^{th} segment
N	number of nodes
$NCON$	number of constraints

* Research Scientist. Member AIAA, AHS.
** Aerospace Engineer, Interdisciplinary Research Office. Member AIAA, AHS.
*** Programmer/Analyst.

NDV	number of design variables
NSEG	number of blade segments
R	blade radius
W	blade weight
W_i	weight of i^{th} segment
W_{NS}	nonstructural weight
W_{NS_i}	nonstructural weight of i^{th} segment
W_S	structural weight
W_{S_i}	structural weight of i^{th} segment
Y	nondimensionalized radial distance
α	prescribed autorotational inertia
λ	taper ratio
ϕ_i	i^{th} design variable
ρ_i	weight density of the i^{th} segment
μ	advance ratio
σ_i	centrifugal stress in i^{th} segment
σ_{max}	maximum allowable stress
ψ	blade azimuth angle
Ω	rotor speed

Subscripts

r	root value
t	tip value
L	lower bound
U	upper bound

Introduction

In recent years structural optimization has become a practical tool which can expedite mechanical design. An extensive amount of work has been done in developing design optimization procedures to bring the state of the art to a high level[1-5]. While these techniques have received wide attention for fixed wing aircraft[1], they are less well known in the rotary wing industry[4-5]. In the past the conventional blade design process was controlled mainly by the designer's experience and by trial and error. Today with improved understanding of helicopter analyses and efficient optimization schemes, attempts are being made to apply design optimization techniques and eliminate the expensive man-in-the-loop iterations.

The helicopter rotor blade design process is multidisciplinary in nature and involves a merging of several disciplines, including structures, aerodynamics, dynamics and acoustics. For example, the blade design must satisfy specified strength criteria and be damage tolerant. The blade must be aeroelastically stable[6,7] and the aerodynamic performance should be optimized[8]. The noise levels generated by the rotor which are a function of local Mach number and airloads must be minimized[9].

An important criterion in rotor blade design has been reduced vibration. For a helicopter in forward flight, the nonuniform flow passing through the rotor causes oscillating airloads on the rotor blades which are translated into undesirable vibratory shear forces and bending moments at the hub. Vibration alleviation therefore plays a major role in the rotor blade design[10]. In the conventional design process this has been accomplished by postdesign addition of lumped/tuning masses which may cause significant increases in the blade weight. Hence an important design consideration is to obtain an optimum blade design for reduced vibration without incorporating a weight penalty[6,11-18].

In most of the work[8,11-15] where optimization techniques were used to address blade design, attempts were made to satisfy certain design requirements and criteria related to a single discipline. The blade design was treated as a series of nearly independent design tasks with little consideration of the couplings and interactions between disciplines. For example, only blade aerodynamic requirements were considered in Ref. 8. In Refs. 11 and 12 only dynamic design requirements were considered in optimum rotor blade designs. Taylor addressed the problem of vibration reduction through modal shaping in Ref. 11. In Ref. 12 Peters' approach was to place the natural frequencies away from the critical frequencies and thereby reduce the hub shear. Blade structural requirements only were considered in Ref. 13. In Refs. 14 and 15 minimum weight designs were presented for articulated rotor blades with rectangular and tapered planforms but in the absence of airloads.

The necessity of merging appropriate disciplines to obtain an integrated design procedure is being recognized. With improved understanding of helicopter analyses, it is now possible to include the couplings between the disciplines in the optimization procedure. Some initial investigations at partially integrating some of these disciplines are presented in Refs. 6 and 16-19. In Ref. 6 the dynamic and aeroelastic requirements were integrated and in Refs. 16-18 the dynamic design requirements were coupled with prescribed airloads in the analysis. Ref. 19 presented a formulation of the integrated procedure involving dynamics and aerodynamics.

Currently at NASA Langley Research Center, there is an effort to integrate various disciplines in the rotor blade design process[20]. The present paper is a part of this effort. The purpose of the present work is to take an initial step in integrated aerodynamic/dynamic optimum design of a rotor blade by coupling two important technical disciplines - blade aerodynamics and dynamics. Design variables affecting both aerodynamics and dynamics are used and coupled aerodynamic and dynamic blade analyses are involved. The coupling is incorporated by including blade airload calculations in the analysis. The airloads change during the optimization process as a function of the design variable values. A trim analysis is part of the procedure and the blade is trimmed at each intermediate design step of the optimization process. This paper concentrates on the low vibration and the low blade weight aspects of the design. The objective of the work is to reduce the blade weight and the 4 per rev (4/rev) vertical hub shear, which is the critical shear force transmitted to the hub by a four-bladed rotor. When both the weight and the shear are simultaneously minimized a multiple objective function technique is needed. A method known as the 'Global Criteria Approach'[21] is used in the present work. The optimization procedure developed is applied to a blade test problem. Results obtained with a multiple objective function formulation are compared with two single objective function formulations - one with the blade weight as the objective function and the other with the 4/rev vertical shear as the objective function.

Problem Description

The design goal is to minimize the weight and the 4/rev vertical hub shear of a rotor blade in forward flight. The constraints are 'windows' on the coupled flap-lag natural frequencies to prevent them from falling into the critical ranges. These windows are selected by careful consideration of the blade frequency versus rotor speed diagram and the associated frequency coalescence points. Constraints are imposed on frequencies of the first four coupled elastic modes. A prescribed lower bound on the blade autorotational inertia and a maximum allowable upper bound on the blade centrifugal stress are also included as constraints.

A linear taper is allowed along the blade planform (Fig. 1). The blade taper ratio, λ, is expressed as follows :

$$\lambda = c_r / c_t$$

where c_r is the root chord and c_t is the tip chord. The design variables are the following: EI_{xx_r}, EI_{zz_r}, GJ_r, λ, c_r, k_r, and w_j (j=2,...,N) where EI_{xx} and EI_{zz} are the bending stiffnesses, GJ is the torsional stiffness, k is the radius of gyration and w_j is the nonstructural weight at the j^{th} node. The subscript 'r' refers to values at the root and N denotes the number of nodes. The lumped nonstructural weight at node 1 is not used as a design variable since it involves contribution from the hub.

Optimization Formulation

Three optimization formulations are studied. The first formulation minimizes the blade weight W, the second minimizes the 4/rev vertical shear F_z and the third minimizes the weight and the 4/rev shear simultaneously. To minimize the blade weight and the 4/rev vertical shear simultaneously, the Global Criteria Approach[21] is used. Using this method the optimum solution is obtained by minimizing a 'global criterion' $F(\phi)$ where

$$F(\phi) = \left(\frac{W(\phi) - W(\phi_1^*)}{W(\phi_1^*)} \right)^2 + \left(\frac{F_z(\phi) - F_z(\phi_2^*)}{F_z(\phi_2^*)} \right)^2$$

subject to (1)

$$g_j(\phi) \le 0 \quad j = 1, 2, ..., NCON.$$

The global criterion is thus defined as the sum of the squares of the relative deviations of the individual objective functions W and F_z from their respective individual optimum values. The design variable vector ϕ_1^* is obtained by minimizing the single objective function $W(\phi)$ subject to the set of constraints $g(\phi)$ and the design variable vector ϕ_2^* is obtained by minimizing F_z subject to the same set of constraints. In Ref. 19 this approach gave good results when minimizing weight and centrifugal stress for a blade in vacuum. However, in the present case, due to the highly nonlinear nature of the above function the following objective function is used

$$\hat{F}(\phi) = \sqrt{F(\phi)}$$

where $F(\phi)$ is given by Eqn. 1.

The three formulations are summarized in Table 1. In this table f_k represents the k^{th} natural frequency where k=3,..,6 (the first two modes are assumed rigid body modes). The subscripts L and U denote lower and upper frequency bounds, respectively. The quantity α is the prescribed lower bound on

the autorotational inertia AI, σ_i is the centrifugal stress on the i^{th} blade segment, σ_{max} is the maximum allowable blade stress, FS is a factor of safety and NSEG denotes the number of blade segments.

Blade Analytical Representation

In this section, expressions for cross sectional properties are presented for the blade model (Fig.1) used in the optimization process. Since the detailed design geometry of the blade cross section is not part of the current work, the cross sectional area and the weight of the blade are formulated in terms of the design variables used. The total blade weight, W, has two components - the structural component W_S and the nonstructural component W_{NS}. The blade weight is:

$$W = \sum_{i=1}^{NSEG} (W_{S_i} + W_{NS_i}) \tag{2}$$

where W_{S_i} and W_{NS_i} are the structural and nonstructural weights of the i^{th} segment respectively. The structural weight of the i^{th} blade segment, W_{S_i}, is

$$W_{S_i} = A_i \rho_i L_i \tag{3}$$

where A_i, ρ_i and L_i denote the segment cross sectional area, the weight density and length respectively. Since the nonstructural weights are specified at the nodes in the test problem the segment nonstructural weight is calculated by averaging the values of these weights at the two associated nodes as follows

$$W_{NS_i} = L_i(w_i + w_{i+1})/2 \tag{4}$$

where w_i denotes the nonstructural weight per unit length at the i^{th} node (Fig. 2).

The expression for the blade cross sectional area contributing to the blade structural weight is developed in terms of the radii of gyration and the stiffnesses as follows. Assuming that the blade is made of isotropic material the moments of inertia of the blade structural component about the z and x axes (Fig.1) are given by

$$I_{xx} = A k_{xx}^2 \tag{5}$$

$$I_{zz} = A k_{zz}^2 \tag{6}$$

where A denotes the cross sectional area and k_{xx} and k_{zz} are the radii of gyration about the z and x axes respectively. The expression for A, obtained by summing Eqns. 5 and 6, is given by

$$A = (EI_{xx} + EI_{zz})/Ek^2 \tag{7}$$

where k (principal radius of gyration) is

$$k^2 = k_{xx}^2 + k_{zz}^2. \tag{8}$$

Assuming that the blade stiffnesses are contributed by the blade structural component only and recalling that the inertia $I \propto L^4$, the distribution of the stiffness EI_{xx} along the blade radius is expressed in terms of its root value as follows

$$EI_{xx}(y) = EI_{xx_r}\left[\frac{y}{R}\left(\frac{c(y)}{c_r} - 1\right) + 1\right]^4 \tag{9}$$

where R is the blade radius, y is the radial location and c(y) is the chord distribution for a linear taper given by

$$c(y) = c_r\left[\frac{y}{R}\left(\frac{1}{\lambda} - 1\right) + 1\right]. \tag{10}$$

Similar expressions are derived for $EI_{zz}(y)$ and GJ(y).

The autorotational inertia (AI) of the blade is calculated from the segment weights as follows

$$AI = \sum_{i=1}^{NSEG} W_i \hat{y}_i^2 \tag{11}$$

where W_i denotes the total weight of the i^{th} segment and $\hat{y}_i$ denotes the distance from the root to the center of the i^{th} segment. The centrifugal stress in the i^{th} segment is calculated as follows

$$\sigma_i = \frac{\sum_{j=i}^{NSEG} W_j \Omega^2 y_j}{A_i} \qquad (12)$$

where σ_i is the stress due to centrifugal forces in the i^{th} segment and Ω is the rotor speed.

Analysis

The optimization procedure with integrated aerodynamics and dynamics is described next. The procedure uses Comprehensive Analytical Model of Rotorcraft Aerodynamics and Dynamics[22] (CAMRAD) for the blade aerodynamic and dynamic analyses. The basic algorithm used for optimization is the method of feasible directions implemented in the program CONMIN[23] along with an approximate analysis.

Aerodynamic Analysis

CAMRAD is used to calculate the section loading from the airfoil two-dimensional aerodynamic characteristics. It uses the lifting line or blade element approach and has corrections for yawed and three-dimensional flow effects[24]. The program also has the provision for including unsteady aerodynamics. It offers two broad categories of trimming - the free flight case and the wind tunnel case. The wind tunnel trim option is selected for this work since the model used in this study is a wind tunnel model of a rotor. The trim option consists of trimming the rotor lift, drag and the flapping angle with collective pitch, cyclic pitch and shaft angle. It is, in fact, a coupled aerodynamic and dynamic procedure. The blade is trimmed for the specified flight condition at each step of the design process. The procedure incorporates the change in planform caused by design variables during optimization.

Dynamic Analysis

The modal analysis of the blade is also performed in CAMRAD which uses a modified Galerkin approach to calculate the mode shapes and frequencies. The method works better than the Rayleigh Ritz approach in the presence of large radial variations of the bending stiffness[24]. Using the airloads information obtained from the aerodynamic analysis the 4/rev vertical shear is calculated.

Optimization Implementation

The optimization procedure is shown in Fig. 3. The process is initiated by identifying the blade preassigned parameters which are held fixed during optimization. The next step is to initialize the design variables and perform the blade structural analysis to calculate the blade properties, the centrifugal stress and the autorotational inertia. The aerodynamic and dynamic analyses are performed next using CAMRAD as described in the previous section. A sensitivity analysis is part of the procedure and consists of evaluations of the derivatives of the objective function and the constraints with respect to the design variables. Analytical derivatives are used for the weight, autorotational inertia and centrifugal stress. Forward finite differences are used for the derivatives of the hub shear and the frequencies. Once the sensitivity analysis is completed optimization is performed.

The optimization process requires many evaluations of the objective functions and constraints before an optimum design is obtained. Therefore an approximate analysis is used along with CONMIN to save computational effort. In the present work, the objective function and constraints are approximated using a piecewise linear analysis that consists of linear Taylor series expansions for the objective function and the constraints. Using CONMIN, along with the approximate analyses, updated design variable values are obtained. The process continues until convergence is achieved. Convergence is checked on the objective function value over three consecutive cycles using a tolerance of 0.5×10^{-5}.

Test Problem

The baseline blade model selected is a wind tunnel blade model of the Growth Black Hawk (GBH)[25] which is a four-bladed rotor. The blade is articulated, has a rigid hub, a linear twist distribution and a distribution of three airfoils along the span. The GBH blade model has rectangular planform for 80 percent of the blade radius and a taper ratio of 3 for the remainder of the blade. The initial CAMRAD model of this blade used 14 aerodynamic segments and 38 structural nodes. Some changes have been made to this model to make it more suitable for the optimization study, e.g., the structural discretization is modified to reduce the total number of design variables. This modified blade model will be referred to as the Modified Growth Black Hawk (MGBH) and has the following modifications

1) the blade is tapered linearly from root to tip,
2) eight structural nodes are used,
3) the same airfoil is used for all aerodynamic segments.

These modifications produce only minimal changes in the aerodynamic and dynamic performance behavior of the blade from that of the GBH blade. This has been verified by performing integrated aerodynamic/dynamic analysis of the two models using CAMRAD. Table 2 contains the parameters of the MGBH and the GBH blades which are fixed during

design optimization. It should be noted that the GBH model rotor has achieved mission requirements in excess of the requirements used in the optimization problem. Therefore the MGBH rotor blade also would satisfy the requirements to begin with though not efficiently. The MGBH blade is used as the starting blade design for the optimization study in the present paper, with a taper ratio of 1, and will also be called the 'reference blade.'

Results and Discussions

This section of the paper presents results from the three formulations summarized in Table 1. The aerodynamic analysis of the blade is performed using CAMRAD with uniform inflow. The blade is in forward flight with an advance ratio, $\mu = 0.30$. The frequency bounds summarized in Table 3. A minimum value α of 19.748 lb-ft^2 is used for the autorotational inertia constraint. An allowable stress σ_{max} of 2.0×10^7 lb/ft^2 and a factor of safety FS = 2 are used.

Results of the three formulations are presented. The effect of optimization on the blade dynamics is assessed by studying the nature of the first four elastic modes associated with the frequencies, f_3 - f_6, constrained during optimization. The effect of optimization on airload distributions is discussed and the total power required by the rotor investigated. In all the optimization results obtained, the center of mass of the blade is forward of the quarter chord point. This is due to the variations of the stiffnesses assumed along the blade radius which do not allow large perturbations of the center of mass. Table 4 summarizes the results obtained using the three formulations. Column 1 presents the reference blade data and columns 2-4 presents the corresponding information for the optimum blades. In the formulations presented here optimum results have been obtained within seven to ten cycles.

Weight Minimization (Formulation 1)

The design obtained using blade weight as the single objective function is presented in column 2 of Table 4. As shown in the table, it is possible to reduce the weight of the blade by 7.5 percent from the corresponding reference blade value while satisfying all the imposed constraints. After optimization, the fourth natural frequency, f_6, is at its prescribed upper bound and the autorotational inertia constraint is at its prescribed lower bound. The optimum blade has a taper ratio of 1.17 and the values of the stiffnesses, EI_{xx_r} and EI_{zz_r}, are increased from their corresponding reference blade values. However, the value of the torsional stiffness at the blade root, GJ_r, remains unchanged after optimization since no constraints are imposed on the blade torsional frequencies. The values of the design variables k_r and c_r are also reduced after optimization. The reduction in the value of c_r reduces the blade area solidity as shown in the table. The value of the 4/rev vertical shear reduces by 40.6 percent from the reference blade value.

Hub Shear Minimization (Formulation 2)

The design with 4/rev vertical hub shear as the single objective function is summarized in column 3 of Table 4. The hub shear is reduced by 85.6 percent compared to the reference blade value. The third coupled natural frequency, f_5, reaches the prescribed lower bound and the autorotational inertia constraint is at its prescribed lower bound. The optimum blade is tapered with the taper ratio 1.18. The values of EI_{xx_r} and EI_{zz_r} are higher than their corresponding reference blade values. The value of GJ_r remains unchanged during optimization for the reason described previously. The values of k_r and c_r are once again reduced after optimization and so is the blade solidity. The total blade weight is reduced by 8.5 percent. The reduction is more significant in this formulation than in the previous formulation where the blade weight is the objective function. This can be explained as follows. The reduction of hub shear reduces the amplitudes of the blade radial airload distribution, as will be shown later, which reduces the blade stiffnesses and thereby reduces the blade weight.

Combined Weight and Hub Shear Minimization (Formulation 3)

Results of the simultaneous minimization of the blade weight and hub shear using the Global Criteria Approach are summarized in column 4 of Table 4. The 4/rev hub shear is reduced by 77.6 percent and the blade weight by 10.6 percent. The constraints are all satisfied and the autorotational inertia constraint is greater than its prescribed lower bound. The optimum blade has a taper ratio of 1.33, which is larger than in the other formulations. The optimum values of the bending stiffnesses EI_{xx_r} and EI_{zz_r} are higher than their respective reference blade values and the value of the torsional stiffness, GJ_r, remains unaltered. The reductions in the value of c_r and therefore in the value of blade solidity are the largest.

Additional Comparisons of Designs

The distributions of the nonstructural weight/unit length for all three formulations, before and after optimization, are shown in Fig. 4. In all formulations the nonstructural weight

increases outboard after optimization due to the presence of the autorotational inertia constraint. The trend is more significant in formulation 2 (hub shear) than in formulation 1 (weight) and is most significant in formulation 3 (weight and hub shear). It is interesting to note that in the hub shear and the multiple objective function formulations, the maximum values of nonstructural weights occur at the next to last node and not at the last node as in the weight optimization formulation. This could be due to some changes in the coupled mode shapes effected by modified stiffness distributions when the hub shear is minimized either separately or simultaneously with the weight. Fig. 5 presents comparisons of optimum weight and vertical shear from all three formulations. Fig. 5a compares the blade weight and Fig. 5b compares the 4/rev vertical shear. As shown in Fig. 5 and Table 4 the Global Criteria Approach provides the lightest blade structure with a hub shear reduction that falls between those obtained from the single objective function optimizations. This is contrary to the intuitive belief that the use of a multiple objective formulation should yield solutions lying between those of the single objective formulations. In other words, the blade weight obtained by simultaneously minimizing weight and hub shear might be expected to be higher than that obtained from weight minimization and the hub shear obtained should be higher than that obtained from hub shear minimization. However, this is only true if the objective functions are monotonically increasing functions of the design variables. This is not true in the present case since for example, the blade weight can decrease with an increase in taper ratio and the hub shear is a very complicated and nonmonotonic function of the design variables.

Effect of Optimization on Mode Shapes

There was a concern that the nature of the mode shapes, corresponding to the frequencies constrained in the optimization procedure, might change as a result of optimization. Therefore the mode shapes for the first four elastic modes are plotted before and after optimization in Figs. 6-9. Part (a) of each figure shows the flapping components and part (b) shows the lead-lag components of the coupled modes. The figures indicate that there is a change in the magnitude of the modal deflections after optimization and in most cases, the node points of the modal deflections are moved slightly outboard from the reference blade. However, no major changes in the nature of the mode shapes occur.

Effect of Optimization on Blade Aerodynamics

Effect on Airloads - Reduction of hub shear is achieved when either of the following occurs: blade natural frequencies move away from the excitation frequencies; mode shapes become more nearly orthogonal to the forcing function or blade harmonic airloads are reduced. It was of interest in the present work to investigate the extent to which the optimization process alters the distribution of airloads.

The influence of the design variables on the section aerodynamic load normal to the plane of the rotor, F_p, is assessed by comparing its radial and azimuthal distributions before and after optimization. Fig. 10 presents the radial distributions of F_p for the advancing blade at $\psi_i = 90$ degree, for both the reference and the optimum blades. Fig. 10 indicates that optimization reduces the amplitude of the vertical airload throughout the span. The reduction is largest in formulation 3. Note that the high negative value of F_p near the tip is caused by the high negative twist of 16 degrees (Table 2) in which the tip of the blade has a smaller pitch angle than the root. Blades with negative twist may carry negative lift outboard and positive lift inboard on the advancing side. It is to be noted that the overall thrust and the propulsive forces are the same for the reference and the optimum blades.

In Figs. 11-13 the azimuthal distributions of the vertical airload, F_p, are plotted for three radial locations. The radial locations selected are near the blade root, at the point of thrust-weighted equivalent chord[26] and near the blade tip. Fig. 11 presents the azimuthal distributions of F_p near the blade root (Y = 0.25, where Y denotes the nondimensionalized radial location). Fig. 12 presents the azimuthal distributions at Y = 0.75 which is the point of occurrence of the thrust-weighted equivalent chord for all the three optimum blades. Fig. 13 shows similar distributions near blade tip (Y = 0.9875). These figures indicate that optimization reduces the amplitudes of the vertical airloads at all three radial locations. Further, formulation 3 produces the maximum reductions. It can therefore be concluded from Figs. 11-13, that the design variables selected for the optimization formulation have significant influence on the amplitude of blade radial and azimuthal distributions of airloads. To complete the investigation the vertical airload distribution nondimensionalized with respect to solidity, F_p/s, is plotted to study the effect of optimization on the vertical blade loading for a given area. Fig 14 shows that the optimum blades produce a larger vertical force for a given area, F_p/s, without stalling, i.e., at any radial location the optimum blades use the area more effectively. The best results are obtained using formulation 3.

Effect on Power Required - Finally, the total power required by the rotor to provide the same amount of thrust is checked before and after optimization. Figs. 10-13 show that optimization not only reduces the amplitude of the vertical airload distributions but it also reduces the peaks and valleys

making the distributions more harmonic both radially and azimuthally. This should indicate a reduction in the total power required by the rotor. Therefore, the power coefficient is calculated before and after optimization. The nondimensional power coefficient C_P/s is shown in Fig. 15 for the reference and the optimum blades. The figure indicates that the total power required to produce the same amount of thrust for a given area reduces significantly after optimization and the reduction is most significant in formulation 3. Hence, optimization improves not only the net rotor power requirement which should reduce since the solidity of the blade is reduced but it also reduces the power per unit area.

Conclusions

In this paper rotor blade designs are generated by use of an integrated aerodynamic/dynamic optimization procedure. Blade weight and 4/rev vertical shear are minimized in the presence of airloads under forward flight conditions using both single and multiple objective functions formulations. Constraints are imposed on the first four coupled natural frequencies (elastic modes only), the blade autorotational inertia and the centrifugal stress. The program CAMRAD is used for the blade dynamic and aerodynamic analyses and the program CONMIN is used for optimization. The Global Criteria Approach is used for the multiple objective formulation and its results are compared with those obtained from single objective function formulations. The optimum designs are compared with those of a reference blade. The optimization scheme used has been very efficient and optimum results have been obtained in seven to ten cycles.

The following observations are made from this study. The Global Criteria Approach for formulating the multiple objective function optimization is very effective. The approach yields a design in which the blade weight is lower than that obtained by using the blade weight as the single objective function due to the nonmonotonicity of the objective functions with respect to the design variables used. The hub shear is somewhat higher than that obtained by using the hub shear as the single objective function. The optimum blades are all tapered in contrast to the reference blade which is rectangular. In all three optimization formulations studied the center of mass of the blade remains forward of the quarter chord point. Inspection of the airload distributions for the initial and the optimum designs indicate that optimization significantly reduces the amplitude and alters the distributions favorably to help achieve the goal of low vibration. The optimization procedure changes the amplitude of the modal deflections and in most cases moves the node points of the associated modes slightly outboard but no significant changes in the nature of the mode shapes occur. Calculation of the total power required by the rotor to produce the same amount of thrust for a given area indicates a significant reduction after optimization.

Acknowledgements

The authors gratefully acknowledge the helpful suggestions of several researchers, in particular, Drs. Henry Jones, Howard Adelman, J. Sobieski and Mr. Matthew Wilbur.

References

1. Ashley, H., "On Making Things the Best - Aeronautical Use of Optimization," AIAA J. Aircraft 19, No. 1, 1982.
2. Sobieszczanski-Sobieski, J., "Structural Optimization Challenges and Opportunities," Presented at International. Conference on Modern Vehicle Design Analysis, London, England, June 1983.
3. Sobieszczanski-Sobieski, J., "Recent Experiences in Multidisciplinary Analysis and Optimization," NASA CP-2327, 1984.
4. Bennett, R. L., "Application of Optimization Methods to Rotor Design Problems," Vertica, Vol. 7, No. 3, 1983, pp. 201-208.
5. Miura, H., "Application of Numerical Optimization Method to Helicopter Design Problems: A Survey," NASA TM-86010, October 1984.
6. Celi, R. and Friedmann, P. P., "Efficient Structural Optimization of Rotor Blades with Straight and Swept Tips," Proc. of the 13th European Rotorcraft Forum, Arles, France, September 1987, Paper No. 3-1.
7. Lim, Joon and Chopra, Inderjit, "Stability Sensitivity Analysis for the Aeroelastic Optimization of a Helicopter Rotor," Proc. of the AIAA/ASME/ASCE/AHS 29th Structures, Structural Dynamics and Materials Conference, Williamsburg, Virginia, April 18-20, 1988.
8. Walsh, J. L., Bingham, G. J., and Riley, M. F., "Optimization Methods Applied to the Aerodynamic Design of Helicopter Rotor Blades," Journal of the American Helicopter Society, Vol 32, No. 4, October 1987.
9. Helicopter Engineering, Part One, Preliminary Design, AMCP 706-201, August 1974.
10. Reichert, G., "Helicopter Vibration Control - A Survey," Vertica, Vol. 5, 1981, pp. 1- 20.
11. Taylor, R. B., "Helicopter Vibration Reduction by Rotor Blade Modal Shaping", Proc. of the 38th Annual Forum of the AHS, May 4-7, 1982, Anaheim, California.
12. Peters, D. A., Ko, Timothy, Korn, Alfred, and Rossow, Mark P., "Design of Helicopter Rotor Blades for Desired Placements of Natural Frequencies," Proc. of the 39th Annual Forum of the AHS, May 9-11, 1983, St. Louis, Mo.

13. Nixon, M. W., "Preliminary Structural Design of Composite Main Rotor Blades for Minimum Weight," NASA TP-2730, July 1987.
14. Chattopadhyay, Aditi and Walsh, Joanne L., "Minimum Weight Design of Rectangular and Tapered Helicopter Rotor Blades with Frequency Constraints," Proc. of the 2nd Int. Conference on Rotorcraft Basic Research, February 16-18, 1988, College Park, Maryland. Also available as NASA TM-100561, February 1988.
15. Chattopadhyay, Aditi and Walsh, Joanne L., "Minimum Weight Design of Rotorcraft Blades with Multiple Frequency and Stress Constraints," Proc. of the AIAA/ASME/ASCE/AHS 29th Structures, Structural Dynamics and Materials Conference, Williamsburg, Virginia, April 18-20, 1988. AIAA Paper No. 88-2337-CP. Also available as NASA TM-100569, March 1988.
16. Hanagud, S., Chattopadhyay, Aditi, Yillikci, Y. K., Schrage, D., and Reichert, G., "Optimum Design of a Helicopter Rotor Blade," Paper No. 12, Proc. of the 12th European Rotorcraft Forum, September 22-25, 1986, Garmisch-Partenkirchen, West Germany.
17. Weller, W. H. and Davis M. W., "Experimental Verification of Helicopter Blade Designs Optimized for Minimum Vibration," Proc. of the 44th Annual Forum of the AHS, June 16-18, 1988, Washington, D. C.
18. Peters, D. A., Rossow, Mark P., Korn, Alfred, and Ko, Timothy, "Design of Helicopter Rotor Blades for Optimum Dynamic Characteristics," Computers & Mathematics with Applications, Vol. 12A, No. 1, 1986, pp. 85-109.
19. Chattopadhyay, Aditi and Walsh, Joanne L., "Structural Optimization of Rotor Blades with Integrated Dynamics and Aerodynamics," Presented at the Second NASA/Air Force Symposium on Recent Advances in Multidisciplinary Analysis and Optimization, Hampton, Virginia, September 28-30, 1988. Also available as NASA TM-101512, October 1988.
20. Adelman, H. M. and Mantay, W. R., "An Initiative in Integrated Multidisciplinary Optimization of Rotorcraft," Presented at the Second NASA/Air Force Symposium on Recent Advances in Multidisciplinary Analysis and Optimization, Hampton, Virginia, September 28-30, 1988. Also available as NASA TM-101523, October 1988.
21. Rao, S. S., "Multiobjective Optimization in Structural Design with Uncertain Parameters and Stochastic Processes," AIAA Journal, Vol. 22, No. 11, November 1984.
22. Johnson, W., "A Comprehensive Analytical Model of Rotorcraft Aerodynamics and Dynamics," Part II: User's Manual, NASA TM 81183, June 1980.
23. Vanderplaats, G. N., "CONMIN - A FORTRAN Program for Constrained Function Minimization," User's Manual, NASA TMX-62282, August 1973.
24. Johnson, W., "A Comprehensive Analytical Model of Rotorcraft Aerodynamics and Dynamics," Part I: Analysis Development, NASA TM-81182, June 1980.
25. Yeager, W., Mantay, W., Wilbur, M., Cramer, R., and Singleton, J., "Wind Tunnel Evaluation of an Advanced Main Rotor Blade Design for A Utility Class Helicopter," NASA TM-89129, September 1987.
26. Gessow, A. and Myers, G. C., Jr., Aerodynamics of the Helicopter, College Park Press, 1985.

Table 1 Summary of the optimization problem

Formulation	1	2	3
Objective function	W	F_z	W and F_z
Constraints	$1 - f_k / f_{k_L}$		k=3,...,6
	$f_k / f_{k_U} - 1$		
	$1 - AI/\alpha$		
	FS $\sigma_i / \sigma_{max} - 1$		(i=1,...,NSEG)
Design variables	EI_{xx_r}, EI_{zz_r}, GJ_r, λ, c_r, r_r, w_j		(j=2,...,N)

Table 2 Growth Black Hawk and Modified Black Hawk blade parameters

Blade radius	4.685 ft
Number of blades	4
Rotational speed	639.5
Flap hinge offset/radius	0.0534
Inplane hinge offset/radius	0.0534
Maximum twist (at blade tip)	-16 degrees
Advance ratio	0.3

Table 3 Blade frequencies (per rev) and bounds (windows)

	Reference	Prescribed bounds	
		lower	upper
f_3	3.068	3.05	3.50
f_4	6.763	6.50	6.90
f_5	9.283	9.25	9.5
f_6	12.632	12.5	12.75

Table 4 Optimization results

	Reference	Formulation 1	2	3
EI_{xx_r} (lb-ft^2)	10277	11305	10306	11818
EI_{zz_r} (lb-ft^2)	354	389.42	384.59	402.15
GJ_r (lb-ft^2)	261	261	261	261
k_r (ft)	0.268	0.192	0.175	0.176
λ	1.0	1.17	1.184	1.33
c_r (ft)	0.450	0.403	0.295	0.281
f_3 (per rev)	3.068	3.194	3.271	3.282
f_4 (per rev)	6.763	6.853	6.87	6.815
f_5 (per rev)	9.283	9.415	9.25	9.487
f_6 (per rev)	12.632	12.750	12.749	12.512
AI (lb-ft^2)	19.748	19.748	19.748	19.955
4/rev hub shear (lb)	0.160	0.095	0.023	0.036
Percent reduction in 4/rev hub shear	–	40.61	85.6	77.6
Blade weight (lb)	3.408	3.152	3.120	3.048
Percent reduction in blade weight	–	7.51	8.5	10.6
Blade solidity	0.122	0.098	0.071	0.062

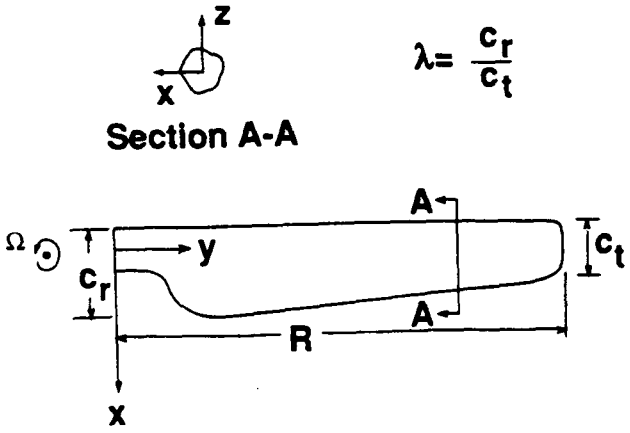

Fig. 1 Simplified rotor blade model with linear taper.

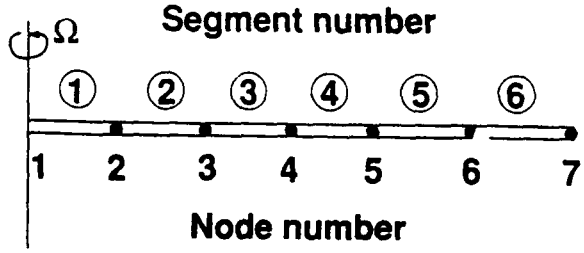

Fig. 2 Discretized blade model.

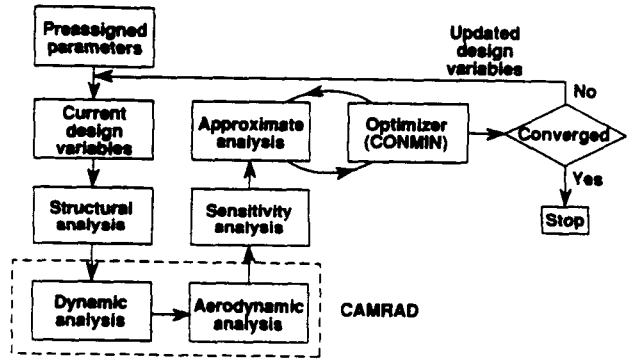

Fig. 3 Flow chart of optimization procedure.

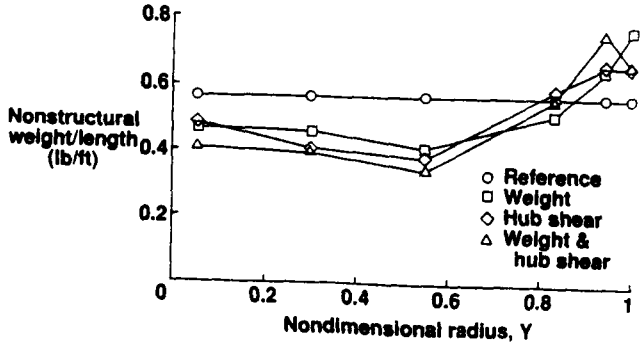

Fig. 4 Nonstructural weight distributions.

ORIGINAL PAGE IS
OF POOR QUALITY

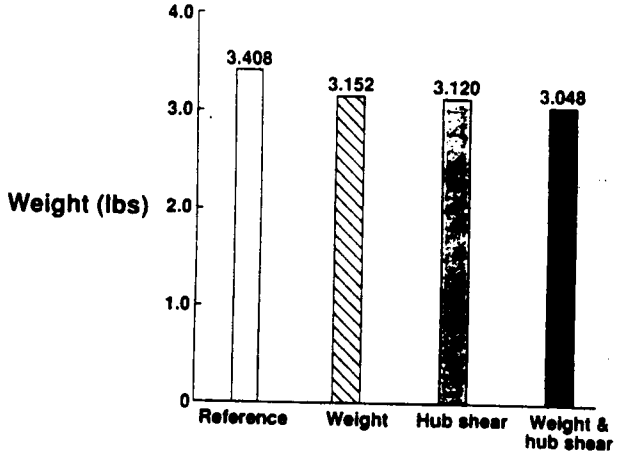

a) Blade weight.

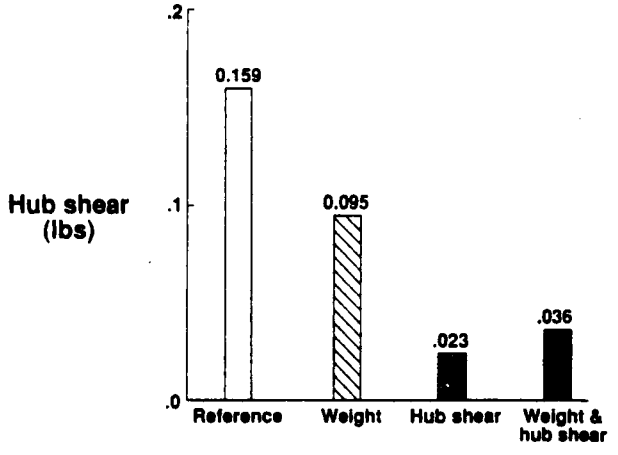

b) 4/rev vertical shear.

Fig. 5 Comparison of optimum weight and hub shear.

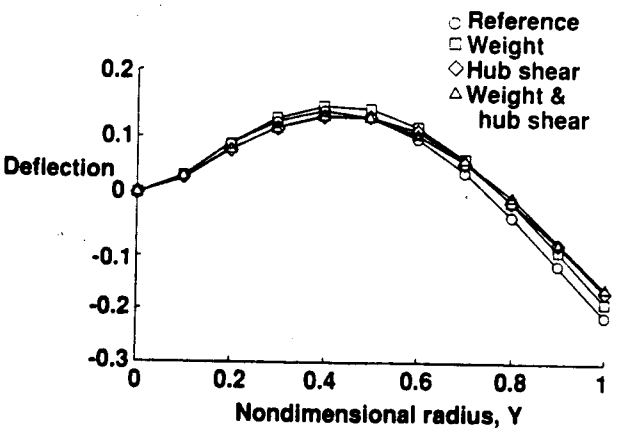

b) Lead-lag deflections.

Fig. 6 Concluded.

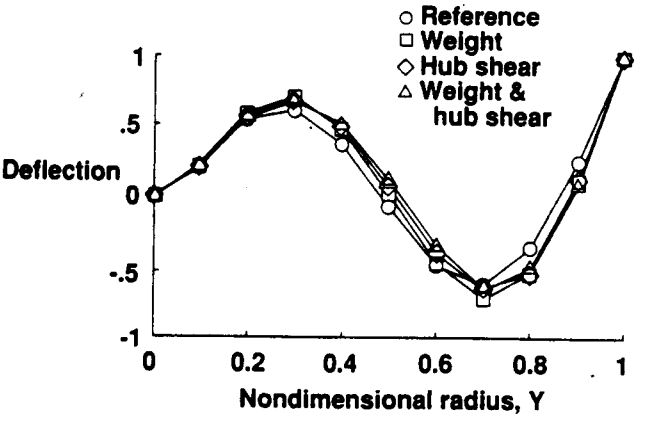

a) Flapping deflections.

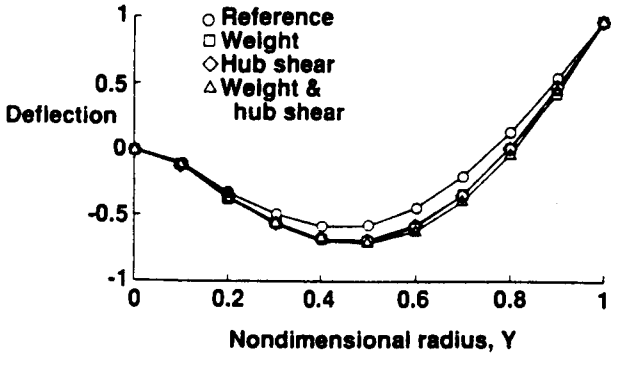

a) Flapping deflections.

Fig. 6 Deflections of first elastic mode.

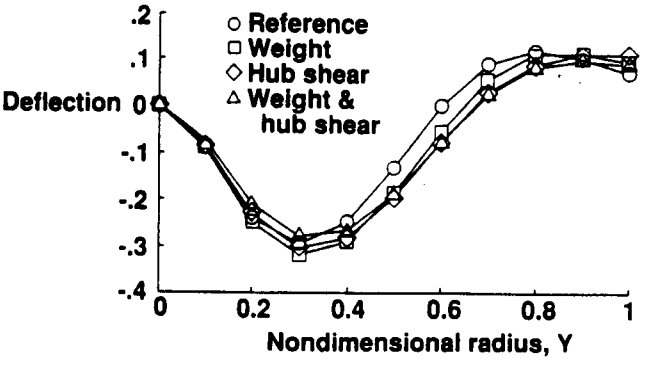

b) Lead-lag deflections.

Fig. 7 Deflections of second elastic mode.

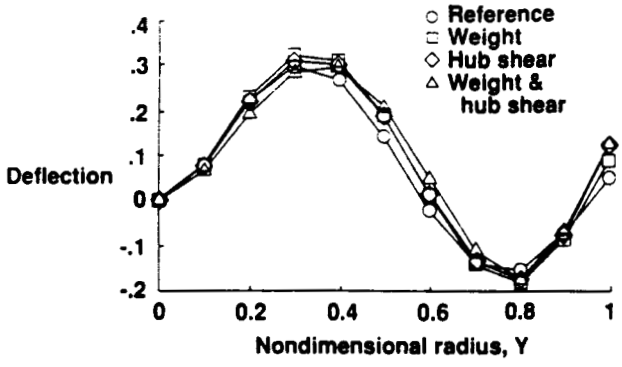

a) Flapping deflections.

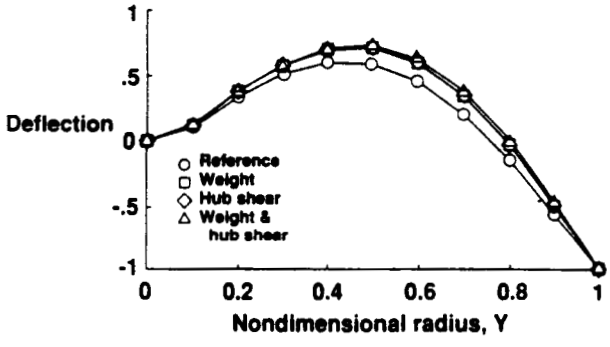

b) Lead-lag deflections.

Fig. 8 Deflections of third elastic mode.

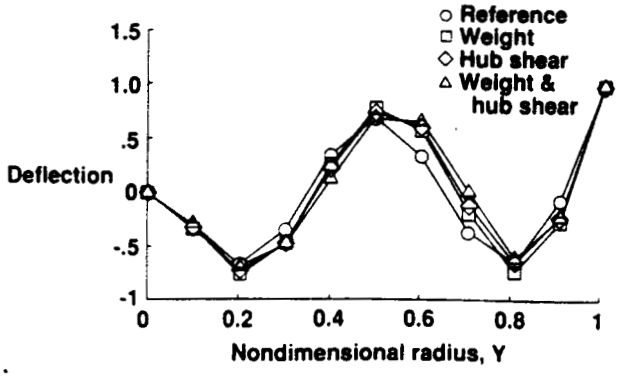

a) Flapping deflections.

Fig. 9 Deflections of fourth elastic mode.

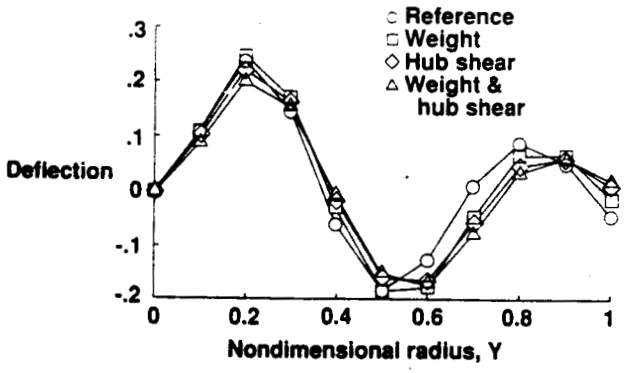

b) Lead-lag deflections.

Fig. 9 Concluded.

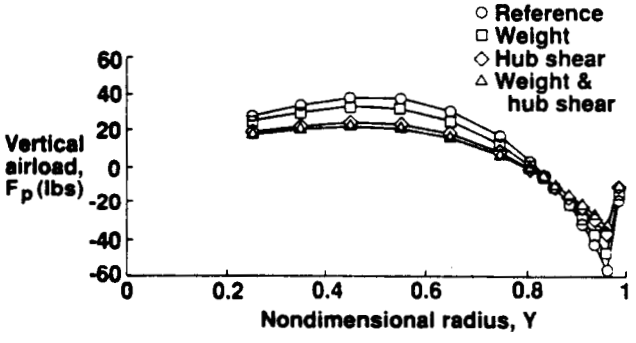

Fig. 10 Radial distributions of vertical airload, F_p; ψ = 90 degrees; μ = .3.

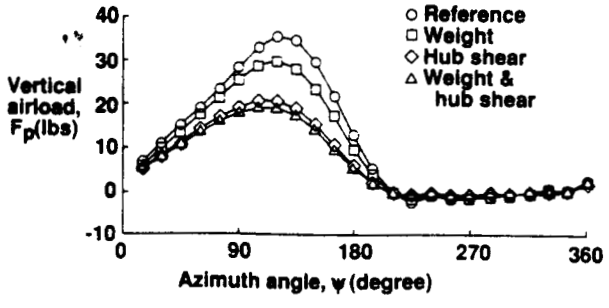

Fig. 11 Azimuthal distributions of vertical airload, F_p; Y = 0.25; μ = .3.

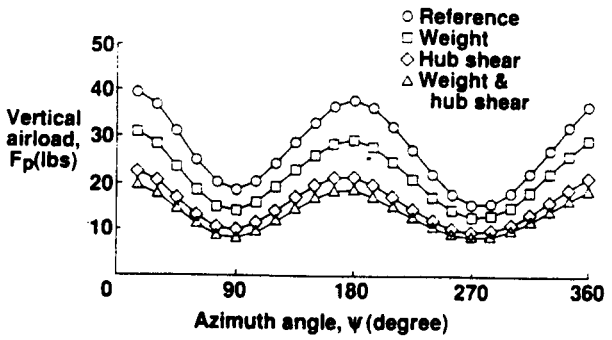

Fig. 12 Azimuthal distributions of vertical airload, F_p; $Y = 0.75$; $\mu = .3$.

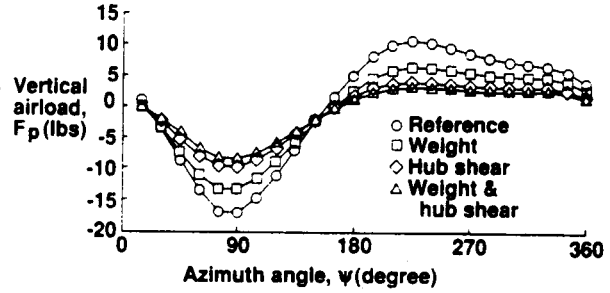

Fig. 13 Azimuthal distributions of vertical airload, F_p; $Y = 0.9875$; $\mu = .3$.

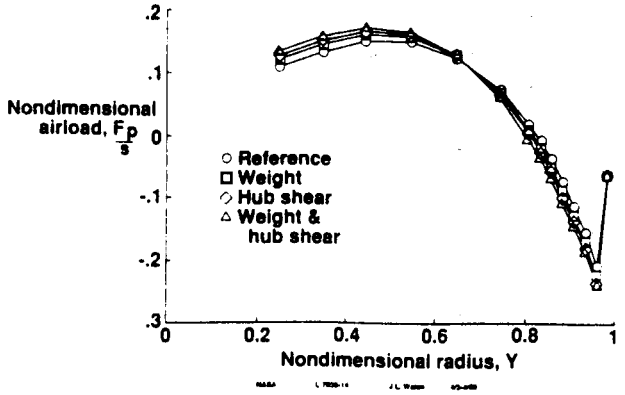

Fig. 14 Radial distributions of nondimensional vertical airload, F_p / s; $\psi = 90$ degrees; $\mu = .3$.

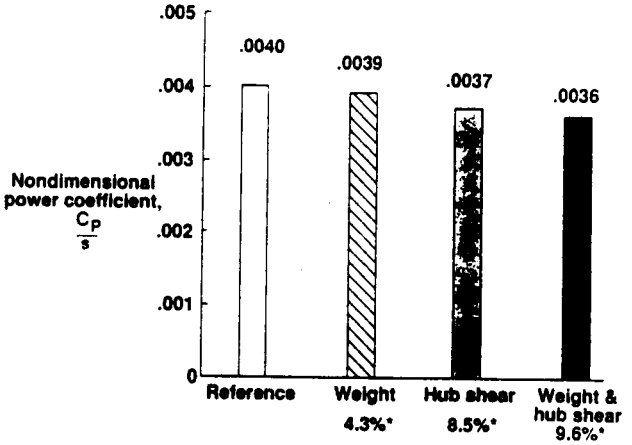

Fig. 15 Comparison of nondimensional power coeffecient, C_P/s.

NASA

Report Documentation Page

1. Report No.	2. Government Accession No.	3. Recipient's Catalog No.
NASA TM-101553		

4. Title and Subtitle	5. Report Date
Integrated Aerodynamic/Dynamic Optimization of Helicopter Rotor Blades	February 1989
	6. Performing Organization Code

7. Author(s)	8. Performing Organization Report No.
Aditi Chattopadhyay, Joanne L. Walsh, and Michael F. Riley	10. Work Unit No. 505-61-51-10

9. Performing Organization Name and Address	11. Contract or Grant No.
NASA Langley Research Center Hampton, VA 23665-5225	13. Type of Report and Period Covered

12. Sponsoring Agency Name and Address	14. Sponsoring Agency Code
National Aeronautics and Space Administration Washington, DC 20546-0001	Technical Memorandum

15. Supplementary Notes

Presented at AIAA/ASME/ASCE/AHS/ASC 30th Structures, Structural Dynamics and Materials Conference, Mobile, AL, April 3-5, 1989.
AIAA Paper No. 89-1269. A. Chattopadhyay, Analytical Services & Materials, Inc., J. L. Walsh, Langley Research Center, and M. F. Riley, Planning Research Corp.

16. Abstract

In this paper, an integrated aerodynamic/dynamic optimization procedure is used to minimize blade weight and 4 per rev vertical hub shear for a rotor blade in forward flight. The coupling of aerodynamics and dynamics is accomplished through the inclusion of airloads which vary with the design variables during the optimization process. Both single and multiple objective functions are used in the optimization formulation. The "Global Criteria Approach" is used to formulate the multiple objective optimization and results are compared with those obtained by using single objective function formulations. Constraints are imposed on natural frequencies, autorotational inertia, and centrifugal stress. The program CAMRAD is used for the blade aerodynamic and dynamic analyses, and the program CONMIN is used for the optimization. Since the spanwise and the azimuthal variations of loading are responsible for most rotor vibration and noise, the vertical airload distributions on the blade, before and after optimization, are compared. The total power required by the rotor (to) produce the same amount of thrust for a given area is also calculated before and after optimization. Results of this study indicate that integrated optimization can significantly reduce the blade weight and the hub shear as well as the amplitude of the vertical airload distributions on the blade and the total power required by the rotor.

17. Key Words (Suggested by Author(s))	18. Distribution Statement
Helicopter Integrated aerodynamics/dynamics Hub shear, blade weight Multiobjective optimization	Unclassified - Unlimited Subject Category 05

19. Security Classif. (of this report)	20. Security Classif. (of this page)	21. No. of pages	22. Price
Unclassified	Unclassified	14	A03